

Enhanced Performance of FH Detection System Using Adaptive Threshold Level

Ammar Abdul-Hamed Khader
Computer Department / College of Engineering
University of Mosul

Abstract

This work investigates the evaluation performance of detection system for Frequency Hopping (FH) signals based on Fast Fourier Transform (FFT) with proposed decision circuit based on Adaptive Threshold Level (ATL), where the threshold level changes its value automatically without manual intervention depending on the estimated values of (SNR) in the channel, the level will be high when the noise is high and vice versus. A comparison in evaluation performance were made with a conventional mode where the decision circuit based on Manually Change Threshold Level (MCTL) done by the detector according to its observation on sensing the Signal to Noise Ratio (SNR). The results shows that the proposed mode (adaptive) is give best results for probability of detection P_D and probability of false alarm P_F comparing with the (Manually Change). Also the results of (adaptive) are compared with that theoretical computation and gives a very small error for high noise while vanish for low noise.

Keyword: Frequency Hopping, Adaptive Threshold Level, Manually Change Threshold Level

تحسين أداء منظومة كشف إشارة القفز الترددي باستخدام مستوى عتبة متكيف ذاتيا

عمار عبد الحميد خضر

مدرس مساعد

قسم هندسة الحاسبات/ كلية الهندسة / جامعة الموصل

الخلاصة

هذا البحث يتناول دراسة تقييم أداء منظومة كشف إشارة القفز الترددي المعتمدة في أساس عملها على طريقة تحويل فورير السريعة FFT والمتبوعة بدائرة اتخاذ قرار مقترحة تعمل على تغيير مستوى العتبة بشكل تلقائي من دون تدخل المستلم وذلك وفقا للتخمين الذاتي المستمر لقيمة الضوضاء المضافة على الإشارة بسبب القناة حيث يرتفع المستوى بارتفاع قيمة الضوضاء وينخفض بانخفاضها. لقد تم فحص وتقييم الأداء مقارنة مع نموذج تقليدي تكون دائرة اتخاذ القرار فيه ذات مستوى عتبة يجب تغييره يدويا من قبل المستلم تبعا لملاحظاته عن تحسس تغير قيمة الضوضاء في القناة. من خلال النتائج العملية تبين أن النموذج الأول المقترح (ذاتي التغيير) أفضل من الثاني (يدوي التغيير) من حيث احتمالية الكشف P_D واحتمالية التنبيه الكاذب P_F . كما تم مقارنة نتائج النموذج المقترح مع النتائج النظرية وكان الفرق بسيط جدا عند قيمة ضوضاء عالية ويتلاشى الفرق عند الضوضاء المنخفضة.

1- Introduction

The communication system designer has other factors to consider besides being able to communicate at a certain range. In the tactical environment shown in Figure (1), intercept receivers and jammers are attempting to compromise the link. The intercept receiver will attempt to non-cooperatively detect the signal of interest (SOI) while the jamming transmitters will attempt to “drown-out” the communication signal through RF interference.

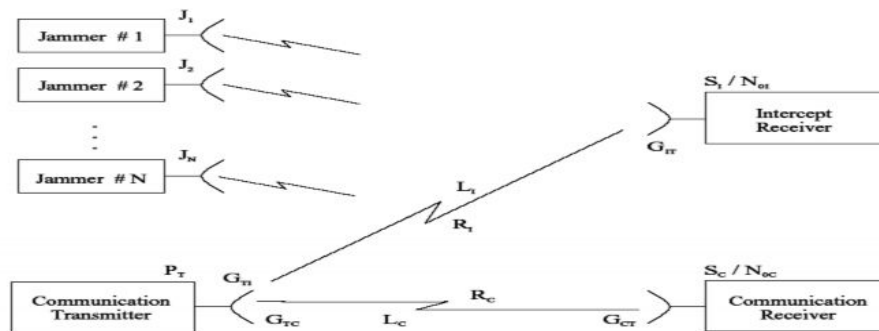


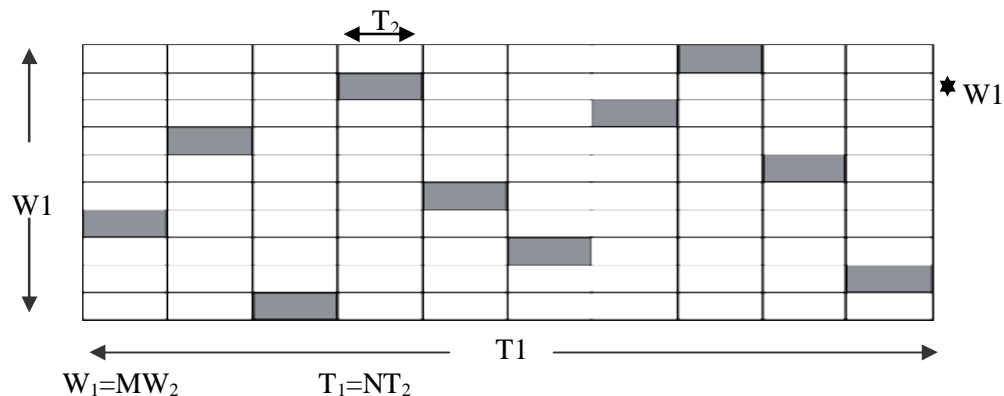
Figure (1): Tactical Communication Scenario

The communication waveform can be manipulated in such a way to make these tasks more difficult. A field of study known as Low Probability of Intercept (LPI) Communications is devoted to designing waveforms that make interception and jamming more difficult. One of the most popular and effective techniques is Frequency Hopping (FH) which is a type of spread spectrum (SS). In a spread-spectrum (SS) system, the transmitted signal is spread over a frequency band that is much larger, in fact, than the maximum bandwidth required to transmit the information bearing (baseband) signal. An SS system takes a baseband signal with a bandwidth of only a few kilohertz (kHz), and spreads it over a band that may be many megahertz (MHz) wide. In SS systems, an advantage in signal-to-noise ratio (SNR) is achieved by the modulation and demodulation process.

The spreading signal is selected to have properties to facilitate demodulation of the transmitted signal by the intended receiver and to make demodulation by an unintended receiver as difficult as possible. These same properties also make it possible for the intended receiver to differentiate between the communication signal and jamming. If the bandwidth of the spreading signal is large relative to the data bandwidth, the spread-spectrum transmission bandwidth is dominated by the spreading signal and is independent of the data signal bandwidth [1].

There are many types of spread spectrum; Direct Sequence (DS), Frequency Hopping (FH), Time Hopping (TH), Chirp (pulsed FM) system and hybrid technique which is a combination of two spread spectrum techniques such as (DS/FH), (TH/FH) and (DS/TH). In FH signals, the signal is transmitted on a certain carrier frequency for a time T_2 . At this time, the carrier frequency will shift (“hop”) to another frequency and stay there for another T_2 , and so on. The number of hops per second is referred to as the hop rate. The communication receiver is synchronized to the transmitter and follows the hopping sequence, whereas an intercept receiver and jammer usually do not. The hopping pattern can be represented graphically in Figure (2). The signal is said to exist for a time of T_1 seconds with a hop duration of T_2 seconds. As the figure indicates, the number of channels is designated M while N is the number of hops in T_1 . Through frequency hopping, the energy of the transmitted signal is effectively “spread” over a BW of W_1 , which is why FH signals are also classified as spread spectrum (SS) signals. An intercept receiver will have to examine the entire signal space

instead of just one carrier frequency to observe the entirety of the signal. In a similar manner, the jamming device, in order to completely disrupt communications, must be able to spread its energy out such that it affects more than just one carrier frequency [2].



Figure(2): FH Signal Space

2- Detection Theory

In detection-theory the simplest detection problem is to decide the presence of a signal or not. The detection of a signal is based on establishing a threshold at the output of the receiver. If the receiver output is large enough to exceed the threshold, a signal is said to be present. On the other hand, if the receiver output is not of sufficient amplitude to cross the threshold, only noise is said to be present. If the condition is noise free and there is no distortion, then we can simply determine the presence of the object by observing the peak in the received signal. However, in real life, noise free condition is impossible [3]. Thus, in the presence of noise or interference, the peaks of the received waveform might be masked by noise, which will make it difficult for us to detect the presence of the object. The presence of noise as might produce erroneous peaks, which might leads to incorrect conclusion [4]. This signal detection problem led us to a binary hypothesis-testing problem. In binary hypothesis-testing problem, we need to decide between two hypotheses, the signal is not present (the observation consist of noise only) or the signal is present (the observation consist of FH signal and noise).

H₀: FH signal is not present

H₁: FH signal is present

Based on these two hypotheses, there are four outcomes that come into consideration. Let D_i as our choice of H_i as the outcome. The decision we made on certain hypothesis will lead us to true or false conclusion as in Table (1) [5] [6].

Table (1): Possibilities of Binary Hypothesis Testing

H_i outcome	D_i choice	Conclusion
H ₀ is the true hypothesis	Decide D ₀	True
H ₁ is the true hypothesis	Decide D ₁	True
H ₀ is the true hypothesis	Decide D ₁	False (Type I Error – False Alarm)
H ₁ is the true hypothesis	Decide D ₀	False (Type II Error – Miss signal)

The above conclusion leads to three main probabilities for performance measures in signal detection problem. There are probability of detection, P_D (decide the FH signal is present when it is), Probability of False alarm (P_F) (decide FH signal is present when it is not) and Probability of Miss (P_M) (decide no FH signal present when it is) [7].

$$P_D = P(D_1 / H_1) = \int_{R_1} f(x / H_1) dx \quad . . . 1$$

$$P_F = P(D_1 / H_0) = \int_{R_1} f(x / H_0) dx \quad . . . 2$$

$$P_M = P(D_0 / H_1) = \int_{R_0} f(x / H_1) dx = 1 - P_D \quad . . . 3$$

3- Detection of FH signals using FFT

The main purpose of the investigation was to choose the best level for threshold to detect a frequency hopped signal in wideband data in the presence of noise.

The received signals at the front-end must be down-converted to the intermediate frequency (IF) domain, a simpler approach is to use a complex mixer before passing the data through the filter. The frequency shift is done so that each channel is shifted in turn to the low-pass filter band. One approach to simplify matched filtering approach is to perform non-coherent detection through energy detection. This sub-optimal technique has been extensively used in radiometry. An energy detector can be implemented similar to a spectrum analyzer by averaging frequency bins of a Fast Fourier Transform (FFT), as in Figure (3).

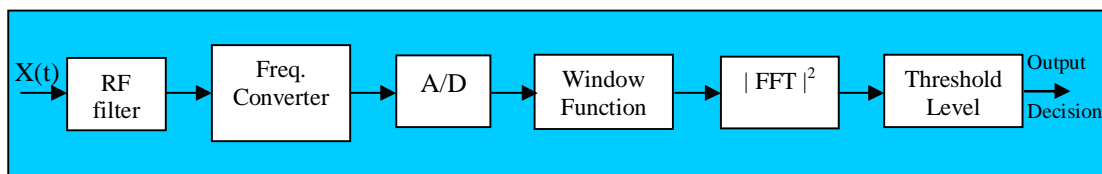


Figure (3): Energy detector

Processing gain is proportional to FFT size N and observation/averaging time T . Increasing N improves frequency resolution which helps narrowband signal detection. Also, longer averaging time reduces the noise power thus improves SNR [8].

Generally, detection performance is related to the size of the observation window (the number of input samples used to make the detection assessment for a given time instance), where longer is better. The best performance is achieved when the observation window matches the hop duration, or when the data containing the entire hop is used to generate a single FFT result, which is then smoothed in frequency. For real time processing, the FFT is a simple and

$$y_k(t) = \sum_{n=0}^{N-1} w(n)x(n+t)e^{-j2\pi kn/N} \quad \text{for } t = 0, N_b, 2N_b, \dots \quad \dots\dots 4$$

attractive choice. Mathematically, the channelized output values can be represented by where N represents the number of samples in each FFT block and is usually chosen so that $N = 2^i$ and i is a positive integer (although variants exist which allow more flexibility in the choice of N), N_b represents the block shift (see Figure 4), $w(n)$ is the windowing function coefficient, $k = 0, 1, \dots, N - 1$ represents the frequency channel number, and the centre

frequency of each channel is given by k/N . Typically the FFT block size will be considerably shorter than the hop duration ($N \ll M$), so assuming a hop signal is present, each sample block will only represent a N/M slice of the hop.

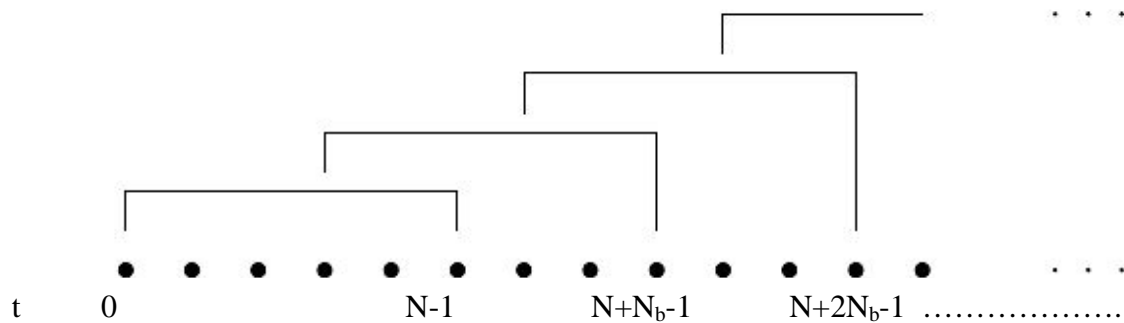


Figure (4): Block shift processing scheme used for channelizing the data. The diagram shows the data (represented by the large dots) divided into overlapping blocks of length N with a shift value of N_b .

The choice of windowing function, represented by $w(n)$, is generally based on reducing the sidelobe level (where high sidelobes lead to interference problems from other in band signals) at the expense of frequency resolution (making it more difficult to resolve signals that are close in frequency).

Detection of hop signals involves finding the values of k where $|y_k(t)|$ exceeds a given threshold. This is repeated for each sample block. Although combining values of $y_k(t)$ from successive blocks could be used to improve the results. Hence the notation can be simplified to

$$y_k = \sum_{n=0}^{N-1} w(n)x(n)e^{-j2\pi kn/N} \dots\dots\dots 5$$

(where the “ t ” has been dropped) since in the statistical development that follows, the results for each sample block of data will be the same.

The hop signal plus noise model was presented in (6).

$$x(n) = aS(n - t_o)e^{j2\pi f_c n} + \sigma v(n) \dots\dots\dots \text{for } n = 0, 1, \dots, N - 1 \dots\dots\dots 6$$

where the following definitions are used:

- N number of samples of wideband data
- t_o hop start time index (i.e. the hop starts at $n = t_o$)
- f_c hop center frequency normalized with respect to the sampling frequency f_s (i.e. $0 \leq f_c < 1$)
- σ real-valued noise amplitude
- $v(n)$ complex noise normalized so that $E\{|v(n)|^2\} = 1$
- a complex-valued signal amplitude
- $S(m)$ complex baseband signal envelope for $0 \leq m < M$ (i.e. during hop) and $S(m) = 0$ for all other values of m . Also normalized so that $E\{|S(m)|^2\} = 1$
- M length of hop in terms of the number of data samples.

In the ideal case being considered, the values of a , t_o , f_c , and σ are all assumed to be unknown. To take into account the band limited nature of a real signal, a modified

representation is used which shows the fundamental frequency components of the hop signal explicitly [9]. It is given by

$$x(n) = \sum_{k=0}^{N-1} a_k e^{j2\pi kn/N} + \sigma v(n) \quad \dots\dots\dots 7$$

where $a_k = 0$ when $f = k/N$ is outside the frequency band of the signal, and

$$\sum_{k=0}^{N-1} |a_k|^2 = |a|^2$$

The objective is to find the peaks in the frequency spectrum which exceed the threshold level. Two modes are examined, the first is Manually Changing Threshold Levels (MCTL) [10] and the second is Adaptive Threshold Levels (ATL).

4- MCTL and ATL

The two modes are based on modelling different parts of the system using MATLAB and examined in AWGN environment. In MCTL mode [10], a threshold used for primary user detection is highly susceptible to unknown because of the ambiguity of SNR value. Due to this reason the thresholds must be adjusted from time to time manually depending on the observation of the receiver, else where the error detection case P_F will be very high and P_D case very small as seems later.

The second mode ATL proposed in this investigation depends on computing the SNR for the received signal, as shown in Figures 5, 6 and 7. The system automatically update its threshold level corresponding to SNR values that computed at the front of receiver and gives a suitable reference. When the noise is high the threshold level will be high, but when it is low the threshold level will be low too. Then the decision circuit at the end of system gives an indication of mark (yes, there is a signal detected), or space (no, signal exist but only noise) which displayed in output port of display, or observing the density of ones on the oscilloscope. Figure (8) and Figure (9) demonstrates the decision output for different values of SNR.

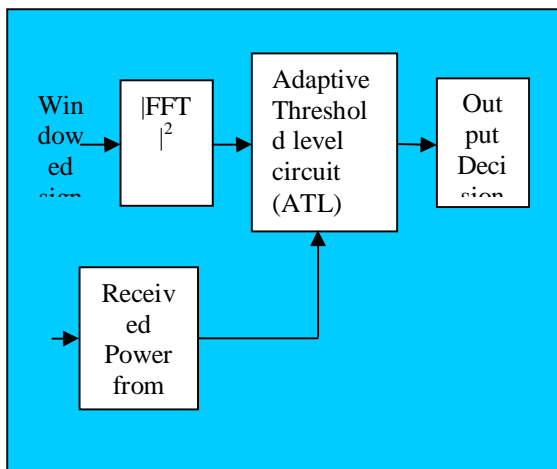


Figure (5): Simulation of FH receiver with adaptive threshold level (ATL)

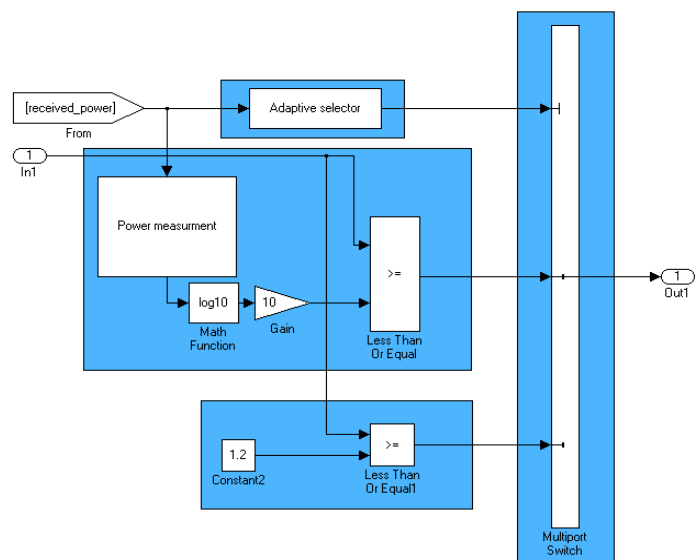


Figure (6): Simulation of adaptive threshold level block (ATL)

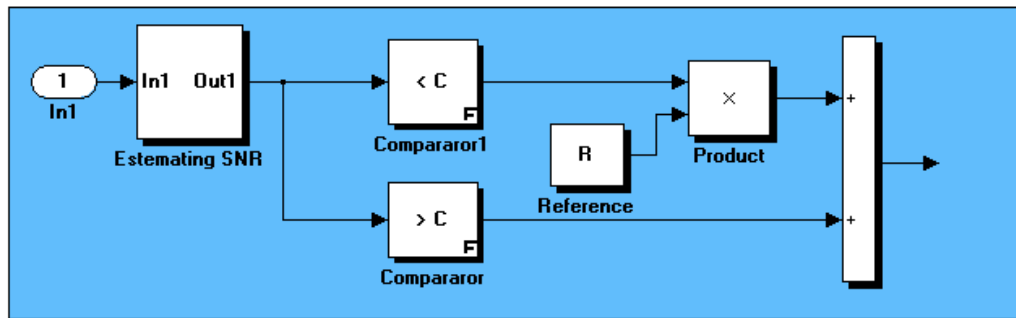


Figure (7): Simulation of Adaptive Selector

5- How decision-making experimentally

The principle of action for the proposed system is guessed the value of SNR for the intercepted signal by measuring the value of its power. To compute the value of SNR, the transmitted power is assumed a 0.78 watt and a noise then added gradually for wide range (from -10 to 10 dB), depending on the value of received power at the intercept system, a different threshold levels are determined and applied to get a lower value for false alarm probability (P_F) and higher value for probability of detection (P_D). Through experience, if the values rang of SNR are between (-10 to -3) dB, the best value of the threshold level is equal to absolute intercepted power value in dB, while when the values rang are between (-2 to 10) dB, the best value of the threshold level is equal to (1.2). Thus the adaptive threshold level system chooses the appropriate level according to the guess value of SNR, so that the threshold level changes its value automatically without manual intervention when the adaptive system sensing any variation in the received power, while in MCTL [10] the change is manually when the interceptor sensing a large amount of (P_F) and this is not efficient method for detection process.

The final decision to know the FH signal is present or not, depends on observing the number of ones and zeros at display or oscilloscope. When the display displays one, this means the FH signal is present, while when it is displays zero, this means no FH signal detected. May be continue appear the ones with split by zeros when the noise ratio is high, in this case the detection process depends on observing the density of ones and zeros to know the FH signal is present or not respectively.

6- The Results

Figure (8) shows that the false alarm probability P_F is much less in ATL mode than MCTL mode where the first strip represent transmitted signals for multi cases (FH signal with noise and noise only (ARROW and STAR respectively)). The second strip denote detected signal using ATL and the third strip for detected signal using MCTL. The percentage number of ones in second strip (ATL) are much less than that in third (MCTL) when only noise signal transmitted (STAR), this means that P_F is larger in MCTL. Another case shown in Figure (9), where the detection probability P_D is better using ATL mode than MCTL because the density of ones is more when FH signal is transmitted (ARROW).

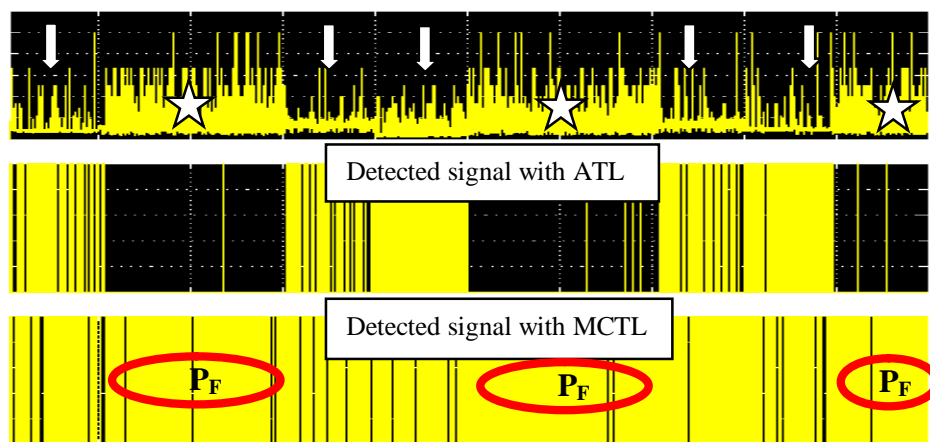


Figure (8): The decision output when SNR= -4 dB

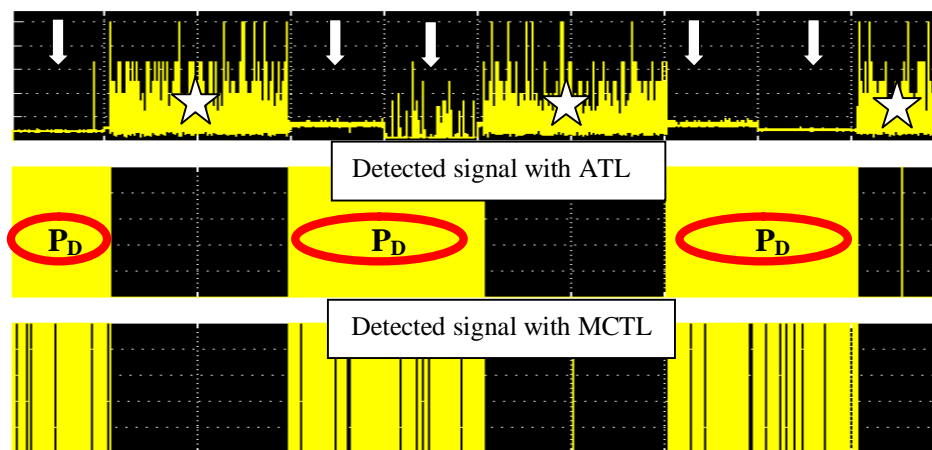


Figure (9): The decision output when SNR= 2 dB

FH signal with noise	↓
Noise only without signal	☆

Table (2) illustrate the percentage number of ones in two modes (MCTL & ATL) for two cases of detection. The first case when there is no hopping signal was transmitted but noise only. Then the ones appears at the output of receiver here is wrong case (P_F), but when the number of ones are decreased an enhancement will done. The enhancement (enh.) of ATL above MCTL from 21 run (from -10 to 10 dB) are 12 case while 6 case are equal (equ.) and 3 case only are degrade (deg.) (from -6 to -4 dB). The second case when there is really FH signal transmitted and received (P_D), the enhancement will done when the number of ones are greater. From 21 run the enhanced in 15 case for one equal case but the degrade in 5 case only (from -10 to -6 dB).

Figure (10) shows the case of Probability of False alarm (P_F) (no hopping signal transmitted), where the number of ones in MCTL is more than that in ATL, unless at SNR (-6.5 to -4) dB. In Figure (11) the test for hopping signal transmitted and received, the percentage number of ones in ATL mode are more than number of ones in MCTL (detection probability P_D is better) unless at SNR (-10 to -6) dB. Note that these results taken based on considering a very correct value of SNR estimated in MCTL case, otherwise the results will be worst. The

simple error cases in ATL mode can be processed by adding multiple comparators, but that will increase the complexity of the system with little enhancements.

Table (2) : The percentage number of ones in MCTL, ATL and the results (enhance, equal and degrade) for FH signal and noise signal

SNR dB	NO FH signal tr.		Results	FH signal tr.		Results
	% No. of 1 MCTL	% No. of 1 ATL		% No. of 1 MCTL	% No. of 1 ATL	
-10	93	29	-64 enh.	95	85	-10 deg.
-9	80	26	-54 enh.	93	85	-8 deg.
-8	75	18	-57 enh.	90	85	-5 deg.
-7	40	14	-26 enh.	90	85	-5 deg.
-6	10	13	+3 deg.	87	85	-2 deg..
-5	8	11	+3 deg.	90	90	0 equ..
-4	7	10	+3 deg.	75	94	+19 enh.
-3	50	3	-47 enh.	92	93	+1 enh.
-2	65	7	-58 enh.	92	95	+3 enh.
-1	55	2	-53 enh.	90	97	+7 enh.
0	20	2	-18 enh.	90	100	+10 enh.
1	15	0	-15 enh.	90	100	+10 enh.
2	8	0	-8 enh.	90	100	+10 enh.
3	5	0	-5 enh.	85	100	+15 enh.
4	1	0	-1 enh.	88	100	+12 enh.
5	0	0	0 equ.	90	100	+10 enh.
6	0	0	0 equ.	93	100	+7 enh.
7	0	0	0 equ.	92	100	+8 enh.
8	0	0	0 equ.	92	99	+7 enh.
9	0	0	0 equ.	93	100	+7 enh.
10	0	0	0 equ.	93	100	+7 enh.

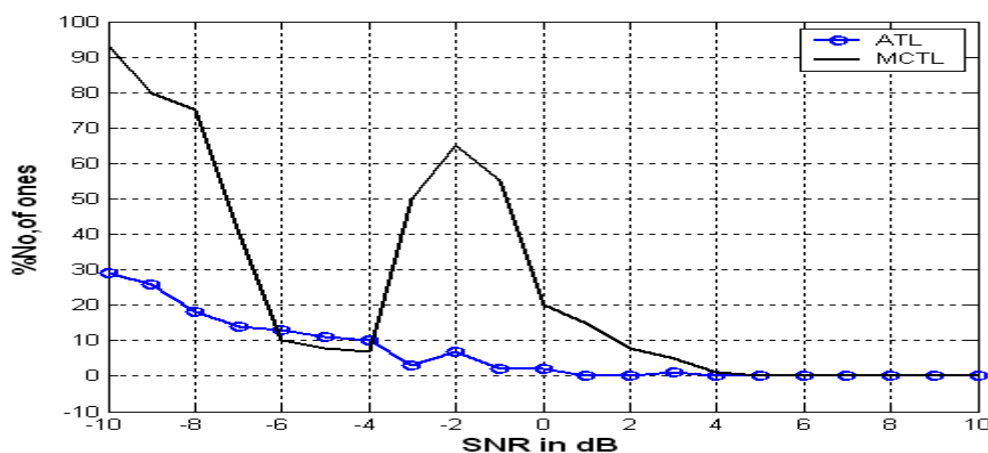


Figure (10): The percentage number of ones for **NO hopping** signal transmitted (P_F) for different SNR

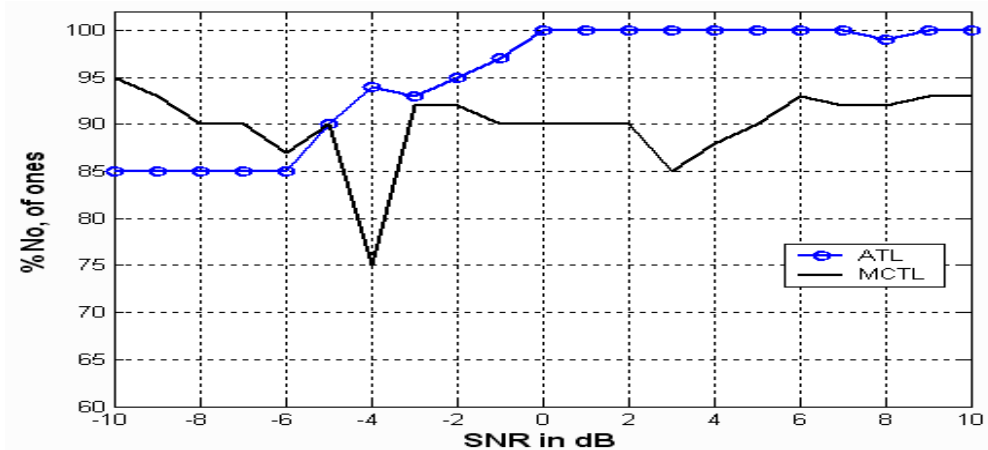


Figure (11): The percentage number of ones for hopping signal transmitted and received (P_T) for different SNR

Figure (12) and (13) shows the enhancement in ATL above MCTL (all values above zero), equally performance case (at zero value) and degradation in detection case (below zero) (ellipse).

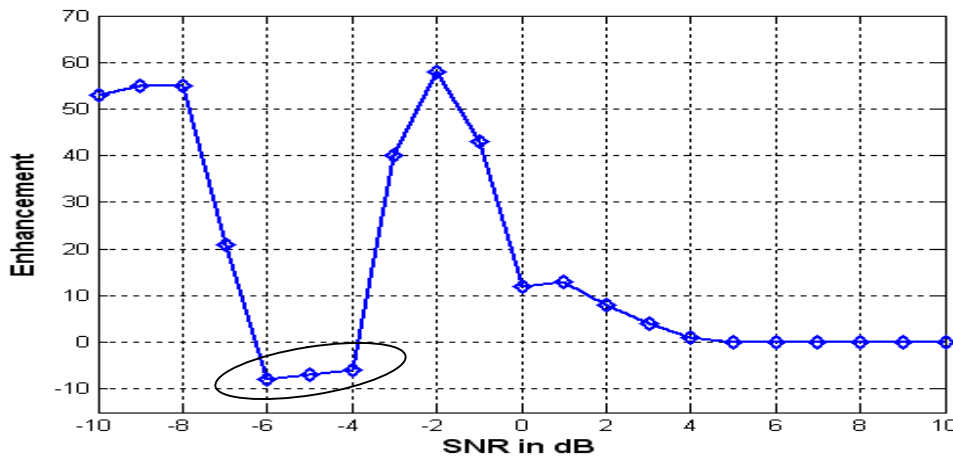


Figure (12): Enhance, equal and degradation performance for NO FH signal transmitted and received (P_F)

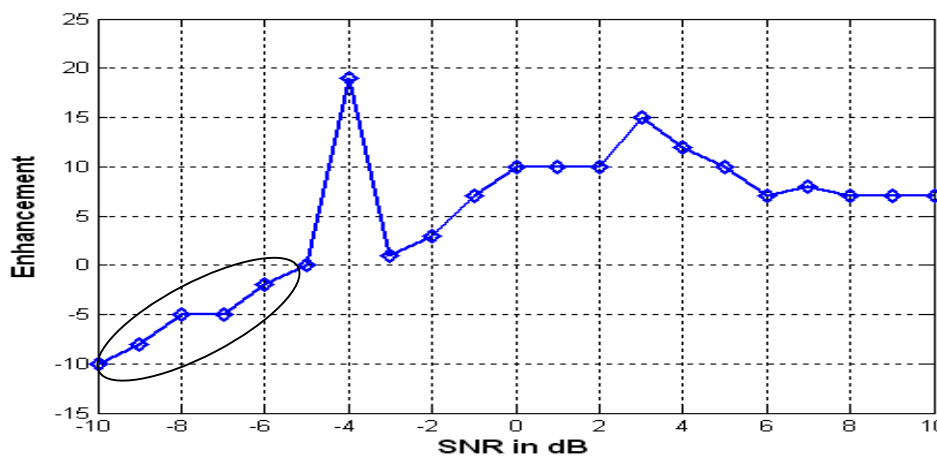


Figure (13): Enhance, equal and degradation performance for FH signal transmitted and received (P_D)

7- Theoretical computation for threshold level in P_F and P_D :

For practical applications, and since it will not necessarily be known whether a sample of data actually contains any hop signals, it is useful to define a threshold. Any peak in $S(t, f)$, where

$$S(t, f) = \sum_{n=0}^{N-1} x(n) s^*(n-t) e^{-j2\pi fn} \dots\dots\dots (8)$$

exceeding this threshold is considered a detection, otherwise it is ignored as being generated by noise effects. The level of the threshold is chosen high enough that noise generated peaks infrequently exceed the threshold, but not so high that signal generated peaks fall below the threshold and do not get detected. Then the probability of false alarm P_F , for a given choice of (t, f) , is given by

$$P_F = e^{-T^2} \dots\dots\dots 9$$

where T is the amplitude threshold level defined relative to the base noise floor of $S(t, f)$ (i.e. the standard deviation of the noise level when no hop signals are present) [9].

Having restricted the definition of the probability of false alarm to P_F , a few comments are in order. The first is that the probability of false alarm drops rapidly as the threshold increases above the noise floor, as shown in Figure (14). If a specific probability of false alarm is desired, then the threshold T can be calculated by rearranging (9) to get:

$$T = \sqrt{-\ln(P_F)} \dots\dots\dots 10$$

An obvious advantage of the definition used here for the threshold (i.e. defined relative to the spectral noise floor), is that for a fixed probability of false alarm, T is independent of M or N [9]. Table (3) shows different threshold values in dB and magnitude values for different SNR and probability of false alarm P_F .

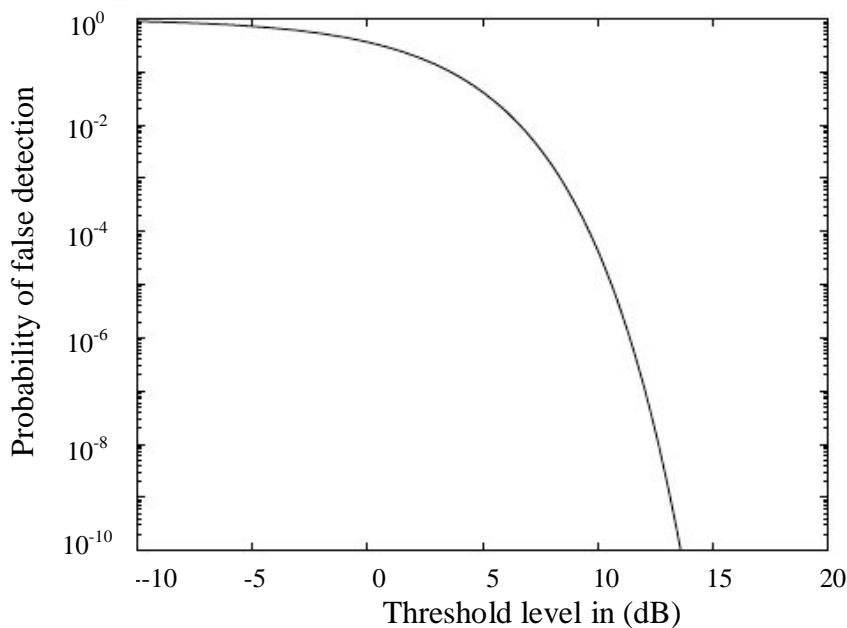


Figure (14): The probability of false alarm as a function of the threshold (measured in dB)

Table (3): Threshold level values for different SNR and P_F

SNR dB	Threshold level for P _F 10 ⁻⁴		Threshold level for P _F 10 ⁻³	
	Absolute	dB	Absolute	dB
-10	8.47	18.56	7.34	17.31
-8	6.73	16.56	5.83	15.31
-6	5.34	14.56	4.63	13.31
-4	4.24	12.56	3.67	11.31
-2	3.37	10.56	2.92	9.31
0	2.68	8.56	2.32	7.31
2	2.12	6.56	1.84	5.31
4	1.69	4.56	1.46	3.31
6	1.34	2.56	1.16	1.31
8	1.06	0.56	0.92	-0.68
10	0.84	-1.43	0.73	-2.68

For detection of a hop signal to occur, the corresponding peak generated in the time/frequency spectrum, S(t, f), must exceed a predefined threshold. The probability of a successful detection is therefore

$$P_D \approx \frac{1}{2} (1 - \text{erf}(\alpha)) + \frac{1}{4\sqrt{\pi M \text{snr}}} e^{-\alpha^2} \left(1 - \frac{\alpha}{4\sqrt{M \text{snr}}} + \frac{1 + 2\alpha^2}{16M \text{snr}} \right) \dots\dots 11$$

where

$$\alpha = \tau - \sqrt{M \text{snr}} \dots\dots\dots 12$$

Some curves representing the probability of detection as a function of SNR, calculated using (11), are plotted in Figure (15). For these curves, various values of the threshold *T* were considered. Inspecting (11) and (12), if (M*snr) remain constant, then the probability of detection will also remain constant. Hence the parameters M and snr are inversely related for a constant probability of detection. Using this fact, the value of the SNR (in dB) can be conveniently represented by the values shown on the X-axis of the plot in Figure (15) minus 10 logM. Note that below 0 dB, the values of the curve for *T* = 5 dB are inaccurate (too high) due to approximation error in (11) [9].

The results in Figure (15) may be combined with the results in (14) to determine detection performance under various conditions. For example, consider the case where the desired probability of false alarm (P_F) is 0.0001, the desired probability of detection is 0.9, and the hop duration is M = 1000 or (30 dB). From Figure (14) the desired threshold *T* is 9.64 dB. Interpolating between *T* = 5 dB and *T* = 10 dB in Figure (15), for P_D = 0.9 the X-axis value is 11.7 dB. Taking into account the effect of M, then the SNR is: 11.7 - 30 = -18.3 dB.

Figure (15) can drawn using matlab program as follows:

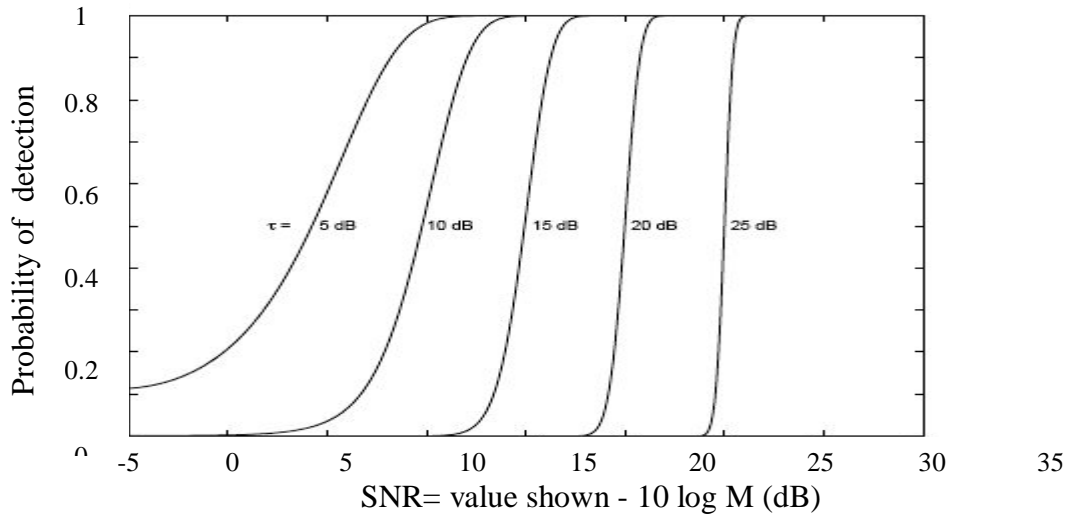


Figure (15): The probability of detection as a function of SNR for various threshold settings

```

for tau_dB =5:5:40; %this value in dB
    tau =10^(tau_dB/20);
    i=0;
    dB_range= -5:35;
    for shown_value=dB_range;
        i=i+1;
        snr =10^(((shown_value-10*log10(m))/10 ))
        alfa =(tau-sqrt(m*snr))
        pd(i) = 0.5*(1-erf(alfa))+[exp(-alfa^2)/(4*sqrt(pi*m*snr))]*
        [1-alfa/(4*sqrt(m*snr))+(1+2*alfa^2)/(16*m*snr)]
    end
    hold on
    plot(dB_range,pd)
end

```

Tables (4) and (5) illustrates the percentage number of ones versus SNR computed as a pure theoretical threshold which is equal to 100% and 0 % respectively, theoretical threshold as in table (3) for $P_F = 10^{-3}$ but applied in simulink and threshold level guessed experimentally in ATL mode, the final field for percentage number of errors for theoretical threshold level applied in simulink and ATL experimental mode, demonstrates the slight difference between them as in Figures (16) and (17).

Table (4): The comparison of percentage number of ones between theoretical and experimental threshold level for P_D case

SNR dB	% No. of ones for multitude threshold level computations for P_D case			% Error between Simu. & Exp.
	Theoretically pure	Theoretical applied in simulink	Experimentally ATL	
-10	100	93	85	8
-8	100	93	85	8
-6	100	93	85	8
-4	100	95	94	1
-2	100	97	95	2
0	100	100	100	0
2	100	100	100	0
4	100	100	100	0
6	100	100	100	0
8	100	100	99	0
10	100	100	100	0

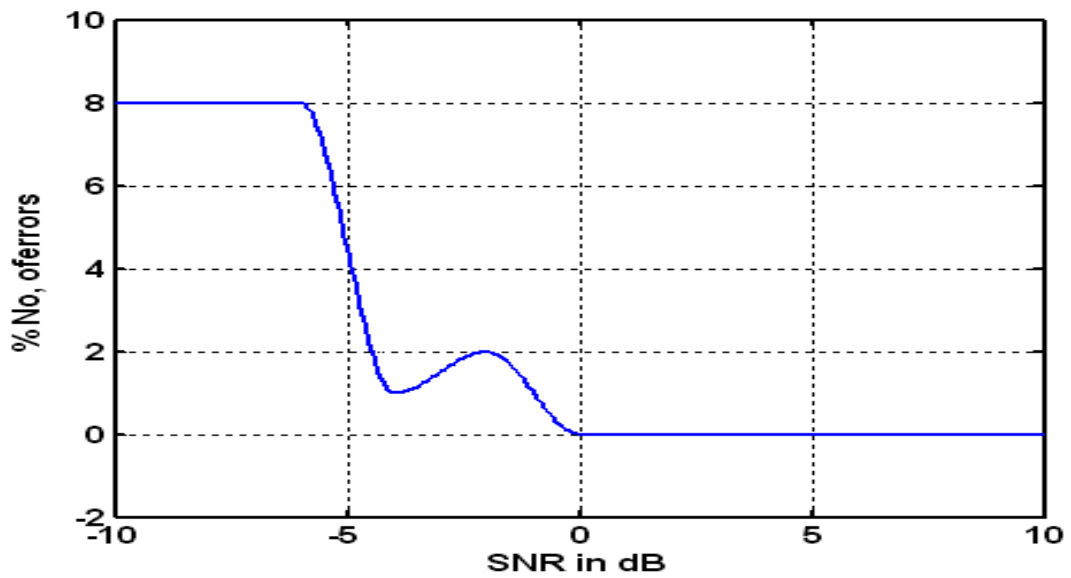


Figure (16): the percentage number of errors for theoretical and experimental threshold level computation versus SNR for P_D case

T

Table (5): The comparison of percentage number of ones between theoretical and experimental threshold level for P_F case

SNR dB	% No. of ones for multitude threshold level computations for P_F case			% Error between Simu. & Exp.
	Theoretically pure	Theoretical applied in simulink	Experimentally ATL	
-10	0	8	29	21
-8	0	8	18	10
-6	0	4	13	9
-4	0	2	10	8
-2	0	1	7	6
0	0	1	2	1
2	0	0	0	0
4	0	0	0	0
6	0	0	0	0
8	0	0	0	0
10	0	0	0	0

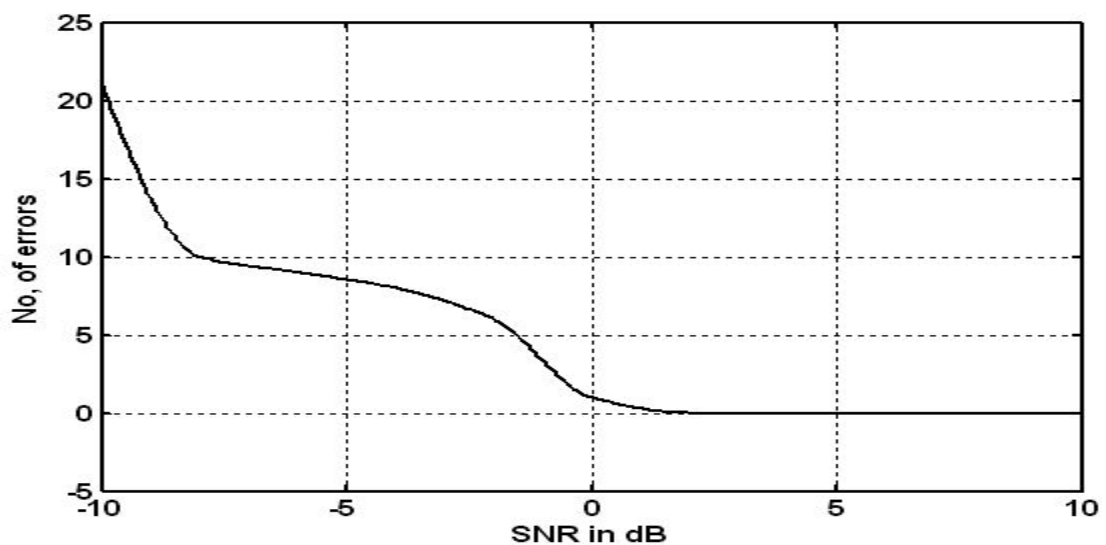


Figure (17): the percentage number of errors for theoretical and experimental threshold level computation versus SNR for P_F case

8- Conclusions

Two simulation models have been used and examined in AWGN environment MCTL and ATL. In ATL mode the threshold levels are varied automatically with variation of SNR computed in receiver. While in MCTL the threshold level is changed manually by the receiver when estimated a large amount of error. From the comparison of results see that ATL performance for P_D (probability of detection) is better than MCTL, while P_F (probability of

false alarm) is less than MCTL mode with a slight error in the two cases. Also there is a slight difference between theoretical and experimental computation for ATL mode for low SNR and that error will vanish when increasing SNR.

9- References

- [1] V. K. Garg "Wireless Communications and Networking" Morgan Kaufmann Publishers © 2007 by Elsevier Inc USA.
- [2] Clint R. Sikes "Non-Cooperative Detection of Frequency Hopping GMSK Signals" M. Sc. Thesis Air University USA\ Air Force Department, March 2006 .
- [3] Robert C. Dixon, "Spread Spectrum Systems with Commercial Application", Feb 1, 2001.
- [4] M. Schwartz and L. Shaw, "Fundamental of Statistical Signal Processing and Estimation Theory", Volume I, 1993.
- [5] G. Hendeby "Fundamental Estimation and Detection Limits in Linear Non - Gaussian Systems" \Ph.D. thesis. Linköping, Sweden 2005.
- [6] A. S. Chon Leong "Performance of Estimation and Detection Algorithms in Wireless Networks" Ph.D. thesis. University of Melbourne Australia Dec 2007.
- [7] N. H. Binti Abdul Aziz "Radar Performance Analysis in The Precence of Sea Clutter" M.Sc. thesis. University of Technology in Malaysia MARCH, 2005
- [8] Danijela C. , Shridhar M. and Robert W. "Implementation Issues in Spectrum Sensing for Cognitive Radios" Berkeley Wireless Research Center, University of California, Berkeley, Conference Record of the Thirty-Eighth Asilomar Conference on Signals, Systems and Computers, 2004.
- [9] William J.L. Read "Detection of Frequency Hopping Signals in Digital Wideband Data" Technical report DRDC Ottawa TR 2002-162 December 2002.
- [10] Ammar. A. Khuder. "Frequency Hopping Signal Detection and Parameter Estimation" M.Sc. thesis. University of Technology Baghdad, December 2004.